ResearchGate

See discussions, stats, and author profiles for this publication at: https://www.researchgate.net/publication/243658730

MAS-NMR Study of Pillared α-Tin and α-Zirconium Phosphates with Aluminum Oligomers

ARTICLE *in* THE JOURNAL OF PHYSICAL CHEMISTRY · FEBRUARY 1995

Impact Factor: 2.78 · DOI: 10.1021/j100005a020

CITATIONS
16

READS
17

6 AUTHORS, INCLUDING:

Enrique Rodriguez-Castellon
University of Malaga
399 PUBLICATIONS **5,337** CITATIONS
SEE PROFILE

Pedro Maireles-Torres
University of Malaga
120 PUBLICATIONS **2,220** CITATIONS
SEE PROFILE

Jesús Sanz
Spanish National Research Council. Instituto …
255 PUBLICATIONS **5,206** CITATIONS
SEE PROFILE

Available from: Pedro Maireles-Torres
Retrieved on: 02 February 2016

MAS-NMR Study of Pillared α-Tin and α-Zirconium Phosphates with Aluminum Oligomers

Enrique Rodríguez-Castellón, Pascual Olivera-Pastor, Pedro Maireles-Torres, and Antonio Jiménez-López*

Departamento de Química Inorgánica, Cristalografía y Mineralogía, Facultad de Ciencias, Universidad de Málaga, 29071 Málaga, Spain

Jesús Sanz*

Instituto de Ciencias de Materiales, C.S.I.C., Serrano 115, 28006 Madrid, Spain

José L. G. Fierro

Instituto de Catálisis y Petroleoquímica, CSIC, Campus Universidad Autónoma, 20049 Madrid, Spain

Received: May 20, 1994; In Final Form: November 14, 1994[⊗]

The nature of the interaction of Keggin-like aluminum oligomers with layered α-tin and α-zirconium phosphates (α-SnP and α-ZrP) has been studied by ^{31}P and ^{27}Al MAS-NMR, complemented with infrared and X-ray photoelectron spectroscopies. According to the type of aluminum solution used, monolayers and bilayers of the tridecamer ion $[AlO_4Al_{12}(OH)_{24}(H_2O)_{12}]^{7+}$ or dimeric polyoxocations, derived from this ion, are intercalated into the layered phosphates. The interaction of the phosphate layer with aluminum species causes a shift of the ^{31}P signal toward high field. The ^{27}Al spectra show the typical resonance lines corresponding to octahedral and tetrahedral aluminum, together with a third resonance at *ca.* 30 ppm assigned to pentacoordinated aluminum, that increases in pillared phosphates formed by calcination at 400 °C. From these results interlayer Al oxide pillars would be cross-linked to the phosphate layer through pentacoordinated Al. The interaction of aluminum with the phosphate layer is stronger in α-ZrP than in α-SnP.

Introduction

The synthesis of pillared layered materials, initially focused on swelling clays as host matrices, has been recently extended to a wide variety of layered hosts.[1−5] Among the pillaring agents, aluminum oligomeric species have been extensively studied as precursors of ceramic oxides and heterogeneous catalysts.[6] Many pillared structures present interesting catalytic properties, showing high selectivities for specific reactions.[7,8]

α-Tin and α-zirconium phosphate (α-SnP and α-ZrP) are two layered solids with the same general formula,[9] α-$M^{IV}(HPO_4)\cdot H_2O$, but with appreciable differences with respect to the intercalation of metal oligomers.[1,10] According to the type of pillaring solution employed,[10] different aluminum oxide-pillared α-SnP materials have been reported, with basal spacing going from 11.5 to 22 Å (gallery free heights, 5−15.5 Å) and specific surface areas of about 200 $m^2\ g^{-1}$. In α-ZrP, stuffed pillared structures seem to be formed,[1] with surface areas below 80 $m^2\ g^{-1}$. Despite that these materials are mainly mesoporous solids, with an internal surface restricted for adsorption, pillared α-SnP derivatives have been successfully used to separate tritiated water,[11] and their exchange capacities[12] are similar to those of smectites. Although these composites were initially designated as alumina-pillared phosphates, assuming that nanostructures similar to that of alumina act as molecular props inside of phosphate galleries, no structural information with respect to the aluminum coordination and aluminum distribution in such materials has been reported so far. Unfortunately, the use of XRD is limited because most of the pillared layered phosphates are long-range disordered.

In the present work, MAS-NMR complemented with other spectroscopic techniques such as X-ray photoelectron spectroscopy (XPS) and infrared spectroscopy (IR) has been used to study the coordination and distribution of Al in the α-SnP and α-ZrP layered phosphates, as well as to determine the nature of the interaction between the aluminum oligomers and the phosphate layers. The textural properties of the aluminum oxide-pillared phosphates are related to the structural arrangement of aluminum.

Experimental Section

Materials. α-ZrP and α-SnP were synthesized following the standard methods previously used.[13,14] Before the intercalation reaction, both phosphates were delaminated with a 0.1 M *n*-propylamine solution[15] at 60% of the saturation capacity. In the case of α-SnP, a further exchange of *n*-propylammonium by tetramethylammonium ions was carried out in order to facilitate the intercalation of the oligomers.[2] Suspensions (1%) of Me_4N−α-SnP or *n*-propylamine−α-ZrP were used for inserting the aluminum oligomeric species.

Three different oligomeric aluminum solutions were employed:[10] Solution I (Al_{13}) was prepared by slow hydrolysis of an 0.2 M $AlCl_3\cdot 6H_2O$ solution with a dropwise-added 0.2 M NaOH solution up to a OH^-/Al^{3+} molar ratio of 1.9 and pH = 4.3. Prior to the reaction, this solution was aged for one month at room temperature. Solution II (CHL) was prepared by dissolving chlorhydrol (Reheis, NJ) in water at an aluminum concentration of 0.08 M. Solution III (Ac) was prepared by dropwise addition of acetic acid to a partially neutralized aluminum solution with NaOH (OH^-/Al^{3+} = 2.5) up to pH = 4.3−4.4. In all cases the amount of aluminum added was between 1.5 and 2 times the cation exchange capacity of the phosphates (6.08 and 6.64 mequiv/g for α-SnP and α-ZrP, respectively).

The intercalation reactions were carried out at room temperature (solutions I and II) or under reflux (solution III), for 1 day. The equilibrium suspensions were centrifuged or, in some

[⊗] Abstract published in *Advance ACS Abstracts,* January 1, 1995.

0022-3654/95/2099-1491$09.00/0 © 1995 American Chemical Society

TABLE 1: Composition, XRD, and BET Surface Area Data of the Studied Samples

sample	Al^{3+} (mmol/g MP_2O_7)[a]	d_{001} (RT) (Å)	d_{001} (400 °C) (Å)	S_{BET} (m^2/g)
Al_{13}–SnP	1.0	17.0	11.8	180
Al_{13}–SnP dial.	2.0	17.1	11.8	
CHL–SnP	2.2	24.6	13.8	190
Ac–SnP	3.3	26.8	20.2	180
CHL–ZrP	5.0	18.9	13.7	75
Ac–ZrP	4.5	29.0	amorphous	70

[a] M = Sn or Zr.

cases, dialyzed. The solids were washed with deionized water and air dried. For comparison a sample of Al^{3+}-exchanged α-ZrP was prepared by putting in contact the suspension of the phosphate with an $AlCl_3$ solution containing a amount of Al equivalent to twice the cation exchange capacity (CEC) of the phosphate.

Techniques. The aluminum content of the samples was determined by atomic absorption spectroscopy. For that purpose, the solids were previously treated under reflux in a 1 M KOH solution. XRD of cast films of powder samples as recorded on a Siemens D501 diffractometer (Cu Kα radiation). Thermogravimetric (TG) and differential thermal analyses (DTA) were carried out on a Rigaku Thermoflex TG 8110 instrument (calcined Al_2O_3 as a reference, and 10 °C min^{-1} heating rate). Adsorption–desorption of N_2 (77 K, outgassing at 200 °C and 10^{-4} mbar overnight) was measured on a conventional volumetric apparatus.

The XPS was recorded with a Fisons ESCALAB 200R with a Al Kα X-ray excitation source ($h\nu$ = 1486.6 eV) and hemispherical electron analyzer. Accurate (±0.2 eV) binding energies (E_B) have been determined with respect to the position of the C 1s peak at 284.9 eV.

The infrared spectra were recorded at room temperature on a Perkin-Elmer 810 spectrophotometer. Self-supporting wafers of the samples with weight-to-surface ratios of about 10 mg cm^{-2} were placed in a vacuum cell assembled with greaseless stopcocks and CaF_2 windows. After outgassing at 200 °C for 1 h, the samples were exposed to pyridine vapor at room temperature for 5 min and then outgassed at room temperature and 350 °C.

^{31}P and ^{27}Al NMR spectra were recorded at 161.98 and 104.26 MHz with a Bruker spectrometer. The external magnetic field used was 9.4 T. All the measurements were carried out at room temperature, and the samples were spun at the magic angle (54° 44′ with respect to the magnetic field) in the range 4–4.5 kHz. ^{31}P and ^{27}Al were recorded after $\pi/2$ (2.6 μs) and $\pi/8$ (2 μs), respectively, and the intervals between successive accumulations (4 and 5 s) were chosen to avoid saturation effects. Solutions of H_3PO_4 and $[Al(H_2O)_6]^{3+}$ were used as external standard references for phosphorus and aluminum chemical shifts.

Results

Starting Materials. The chemical composition, basal spacing, and BET surface area of the studied samples are listed in Table 1. The Al_{13} oligomer solution gives rise to an intercalation compound, Al_{13}–SnP, with an interlayer distance of 17.0 Å. If the equilibrium suspension is dialyzed instead of being centrifuged, the basal spacing is practically the same, but the amount of aluminum retained is higher.

The use of the chlorhydrol solution leads to materials with higher aluminum contents and different basal spacings for each phosphate, 24.6 and 18.9 Å for CHL–SnP and CHL–ZrP,

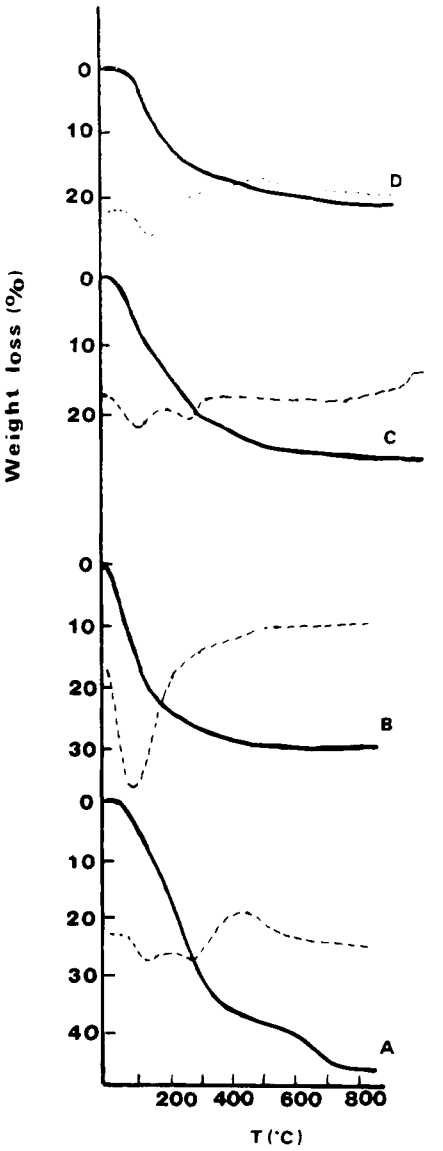

Figure 1. TG and DTA curves of (A) chlorhydrol; (B) Al_{13}–SnP; (C) Ac–SnP; (D) Al_{13}–SnP calcined at 400 °C.

respectively. Note that CHL–ZrP, with a content of aluminum more than twice, presents a lower basal spacing than CHL–SnP, which anticipates a differential behavior of those two phosphates, despite that the CECs are quite similar.

The effect of temperature on the intercalation process has been assessed using solution III under reflux. The Al content and the basal spacing of the sample obtained by the reflux method, Ac–SnP, are much higher than for the other aluminum oligomers–SnP intercalates (Table 1). Thus, the basal spacing of the sample Ac–SnP (26.8 Å) is 9.8 Å higher than that of Al_{13}–SnP. Sample Ac–ZrP exhibits the highest basal spacing (29 Å).

In Figure 1, the TG/DTA curves of representative intercalates of α-SnP are compared with those of chlorhydrol. Apart from the different water contents, these curves show that between 200 and 400 °C the OH^- groups are removed differently in Al_{13} (Figure 1B) and CHL intercalates than in Ac–SnP (Figure 1C). The DTA curve of sample Ac–SnP exhibits, as for chlorhydrol (Figure 1A,C), two distinctive endotherms, at 95 and 250 °C, which correspond to the loss of zeolitic water and OH^- groups, respectively. For samples Al_{13}–SnP (Figure 1B) and CHL–SnP (not shown here) the endotherm at 250 °C is not observed.

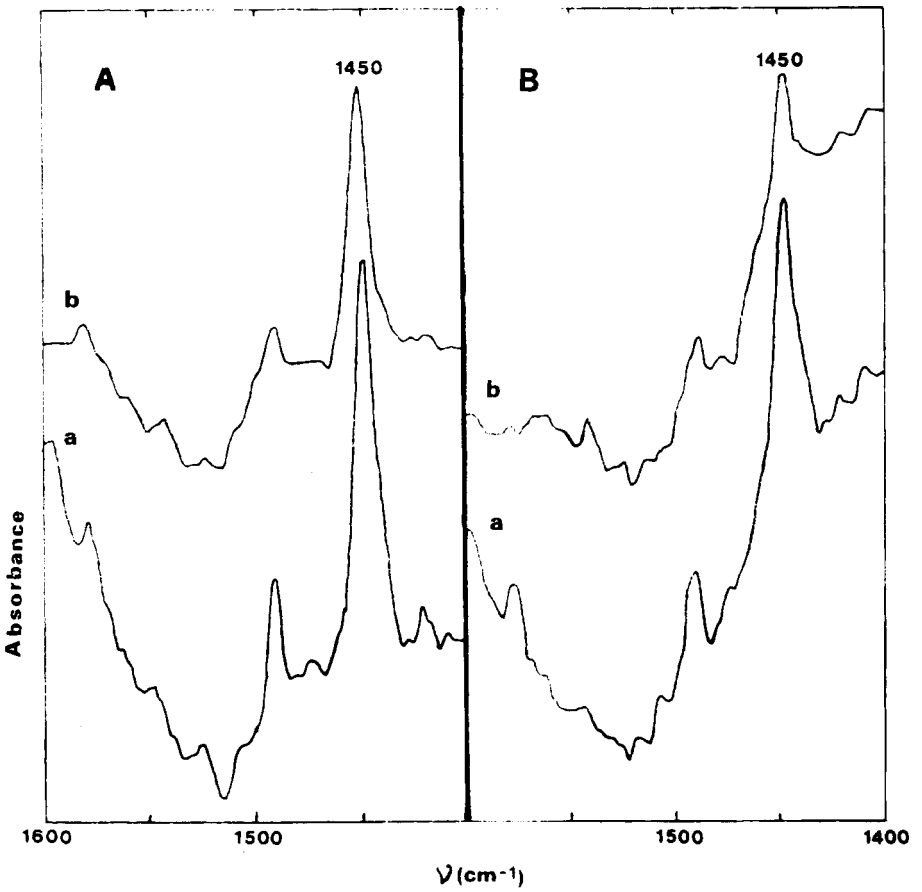

Figure 2. IR spectra of pyridine adsorbed on aluminum oxide-pillared phosphates: (A) Al_{13}–SnP (a) evacuated at room temperature, (b) evacuated at 350 °C; (B) CHL–ZrP (a) evacuated at room temperature, (b) evacuated at 350 °C.

Calcined Materials. Calcination at 400 °C leads to several pillared materials with different basal spacings (Table 1). Whereas the values of the basal spacing of CHL–SnP and Al_{13}–SnP are close (13.8 and 11.8 Å, respectively), the basal spacing of sample Ac–SnP is much higher (20.2 Å), suggesting that bigger polymers than Al_{13} can be accommodated in the phosphate interlayers, when the reflux method is used. In contrast to the behavior observed in Al-pillared clays, where no modification of the basal spacing occurs, a reduction of the basal spacing by about 5 Å is detected in aluminum oxide–pillared phosphates, which may be attributed to the loss of two water molecules as a consequence of the linking of the oligomer with adjacent layers.

All these aluminum oxide-pillared materials are mesoporous solids with a small contribution of micropores. Only slight variations in the pore size distribution are observed.[10] The α-SnP pillared materials have practically the same BET surface area (180–190 m^2/g), showing no dependence at all on the aluminum content and the size/nature of the intercalated oligomer. The BET surface area of the pillared samples of α-ZrP is lower (70–75 m^2/g), indicative of stuffed pillared structures. After calcination, the pillared materials absorb abundant water (Figure 1D), which is characteristic of porous solids.

Figure 2 shows the IR spectra of two representative pillared samples with pyridine adsorbed at room temperature. An intense band appears in these spectra at 1450 cm^{-1}, characteristic of Lewis acid sites, whilst the presence of Brönsted acid sites, near 1550 cm^{-1}, is practically not detected, which indicates that metal ions deficiently coordinated are present on the surface of these materials. These Lewis acid sites are quite strong, as pyridine still remains coordinated at 350 °C.

The XPS technique has been applied to determine the concentration and coordination[16] of aluminum at the surface of the pillared materials, which is of great interest to understand their catalytic behavior. Table 2 lists the binding energies of O_{1s}, Al_{2p}, P_{2p}, and $M(IV)_{3d_{5/2}}$ and the surface chemical composition. In general, the concentration of aluminum on the surface increases with the bulk concentration of aluminum in α-SnP derivatives with Al/Sn ratios between 0.768 and 2.300, whereas in α-ZrP derivatives the Al/Zr ratio is between 2.040 and 2.350. The Al/P surface ratio of both phosphates is very high, but whilst in α-ZrP derivatives it is close to 1, in α-SnP derivatives it oscillates between 0.586 and 1.593.

The chemical environment of aluminum on the surface can be distinguished by using the modified Auger parameter (α′), obtained by the following equation:[17]

$$\alpha' = 1486.6 + KE(Al_{KLL}) - KE(Al_{2p})$$

where $KE(Al_{KLL})$ is the kinetic energy of the Auger electron and $KE(Al_{2p})$ is the kinetic energy of the photoelectron Al_{2p}. The value 1486.6 eV is the energy of the excitation source.[17]

Figure 3 shows the X-ray-induced Al_{KLL} Auger line for different Al-pillared tin phosphates (i.e. materials calcined at 400 °C). The α′ values of aluminum in the pillared phosphates (Table 3) vary between 1460.9 and 1461.3 eV, which are intermediate between 1460.3 and 1460.6 eV for tetrahedral coordination and 1461.3–1461.5 eV for octahedral coordination of well-known aluminosilicates.[16] α′ values in the range 1460.9–1461.3 eV have been assigned to octahedral Al in dealuminated zeolites.[18]

^{31}P MAS-NMR. Figures 4 shows the ^{31}P MAS-NMR spectra of α-SnP and α-ZrP, together with those of aluminum oligomer

TABLE 2: Binding Energies (eV) and Surface Chemical Composition of Aluminum Oxide-Pillared Phosphate Materials Calcined at 400 °C

sample	O_{1s}	Al_{2p}	P_{2p}	$M^*_{3d_{5/2}}$[a]	Al/M* surface	Al/P surface
Al_{13}–SnP	531.1	74.1	133.2	486.7	0.768	0.586
Al_{13}–SnP dial.	531.2	74.0	133.2	486.6	0.980	0.731
CHL–SnP	531.2	73.9	133.1	486.6	2.300	1.465
Ac–SnP	531.2	73.9	133.2	486.6	2.215	1.593
CHL–ZrP	531.3	74.1	133.2	182.5	2.040	0.949
Ac–ZrP	531.1	74.0	133.2	182.5	2.350	1.000

[a] M* = Sn or Zr.

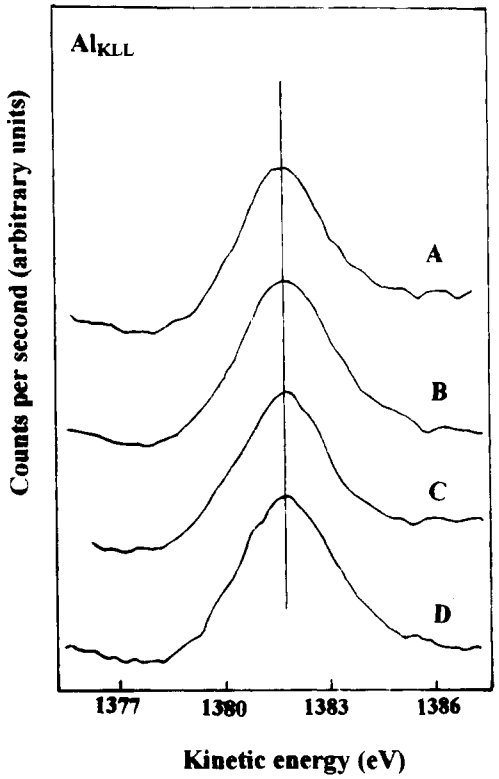

Figure 3. X-ray-induced Al_{KLL} Auger line for different Al-pillared tin phosphates (A) Al_{13}–SnP dial. (B) CHL–SnP, (C) Al_{13}–SnP, and (D) Ac–SnP.

TABLE 3: Kinetic Energies of Al_{2p} and Al_{KLL} and Modified Auger Parameter of Al in Aluminum Oxide-Pillared Materials Calcined at 400 °C

sample	KE Al_{2p} (eV)	KE Al_{KLL} (eV)	α′ (eV)
Al_{13}–SnP	1406.3	1380.6	1460.9
Al_{13}–SnP dial.	1407.0	1381.5	1461.1
CHL–SnP	1407.8	1382.4	1461.2
Ac–SnP	1407.3	1382.0	1461.3
CHL–ZrP	1408.5	1382.9	1461.0
Ac–ZrP	1408.7	1383.2	1461.1

intercalated samples. For comparison the spectrum of an Al^{3+}-exchanged α-ZrP sample is also included.

The spectra of α-SnP (Figure 4A) and α-ZrP (Figure 4F) have been reported previously by Hudson and Workman.[19] The data obtained here corroborate these results. Indeed, the ^{31}P chemical shifts (δ) of α-SnP and α-ZrP are −12.5 and −18.8 ppm, respectively. The spectra of Al_{13}–SnP and CHL–SnP intercalates (Figure 4,B,C,D) show an intense peak centered around −16.0 ppm and a shoulder near −12.0 ppm, which can be assigned to phosphate groups interacting with the aluminum oligomer (type 2) and to the remaining POH groups (type 1), respectively. In the spectrum of Al_{13}–SnP, the intensity ratio I_2/I_1 is 1.50, indicating that only three-fifths of the phosphate

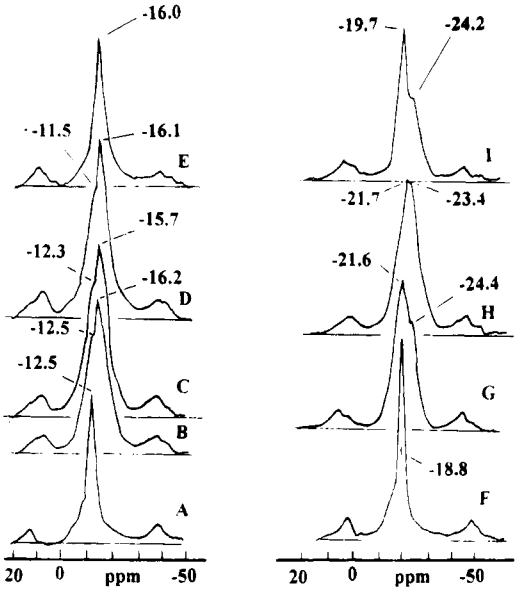

Figure 4. ^{31}P MAS-NMR spectra of α-SnP, α-ZrP, Al^{3+}-exchanged α-ZrP, and aluminum oligomer intercalated α-SnP and α-ZrP: (A) α-SnP; (B) Al_{13}–SnP; (C) dialyzed Al_{13}–SnP; (D) CHL–SnP; (E) Ac–SnP; (F) α-ZrP; (G) Al^{3+}-exchanged α-ZrP; (H) CHL–ZrP; (I) Ac–ZrP.

groups interact with the oligomer. This ratio slightly increases in the spectra of dialyzed Al_{13}–SnP and CHL–SnP (1.86) samples, which is consistent with the presence of increasing amounts of aluminum in the interlayer space of the phosphate. From these spectra, it also appears that the interaction with the Al oligomer produces a shift of the line toward higher field positions, due to an increase of the cation charge around the phosphorus tetrahedra.

When the aluminum oligomeric solution is buffered with acetate and the intercalation reaction is performed under reflux, only one peak, at −16.0 ppm, is observed in the ^{31}P NMR spectrum of sample Ac–SnP (Figure 4E), which suggests that all the phosphate groups of the layer interact with the intercalated aluminum oligomer. This is the material, in the series of α-SnP intercalates, with the highest amount of aluminum taken up (3.3 mmol Al/g SnP_2O_7) and the highest interlayer distance (26.8 Å).

The ^{31}P NMR spectrum of Al^{3+}-exchanged α-ZrP is formed by two shifted components, at −21.6 and −24.4 ppm, associated with two types of P-tetrahedra, indicating that all the P-tetrahedra in α-ZrP are affected by the intercalation of Al^{3+} (Figure 4G). In the case of the CHL–ZrP intercalate (Figure 4H), two signals with similar intensities are resolved at −21.7 and −23.4 ppm. In contrast with what occurs in Ac–SnP, the ^{31}P NMR spectrum of sample Ac–ZrP (Figure 4I) shows two signals, at −19.7 and −24.2 ppm, the former being more intense than the latter. In α-ZrP derivatives, the increase of the chemical shift of the second signal (−4.5/−5.4 ppm) is higher than that of their α-SnP homologues (−3.6/−4.5 ppm), suggesting that the interaction of the intercalated aluminum oligomers is stronger in α-ZrP.

Upon calcination at 400 °C, aluminum oxide-pillared materials are obtained by dehydration of the interlayered oligomers. An additional shift toward higher field is observed in all cases (Figure 5), indicating an increase of the interaction of the phosphate with the aluminum species as a consequence of the thermal transformation experimented by the oligomer. Broad bands centered at −18.2 and −19.1 ppm appear in the spectra of the samples Al_{13}–SnP and CHL–SnP, respectively, whilst the spectrum of the sample Ac–SnP shows a band at −16.6 ppm, together with a shoulder at −22.0 ppm. The signal of

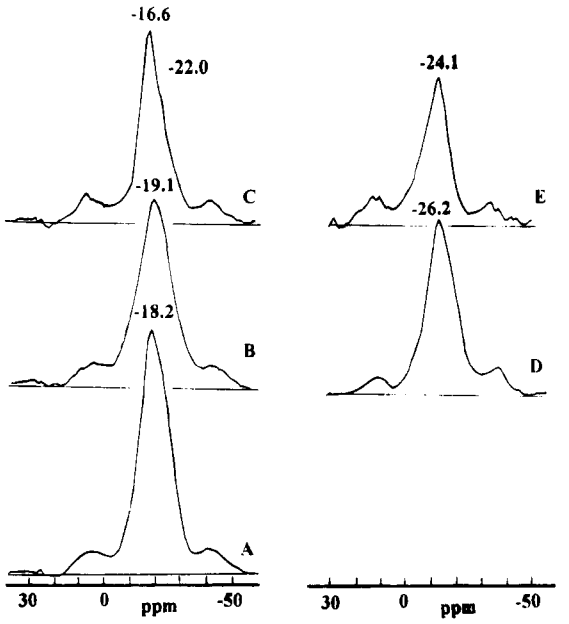

Figure 5. ^{31}P MAS-NMR spectra of aluminum oxide-pillared α-SnP and α-ZrP materials (400 °C): (A) dialyzed Al_{13}−SnP; (B) CHL−SnP; (C) Ac−SnP; (D) CHL−ZrP; (E) Ac−ZrP.

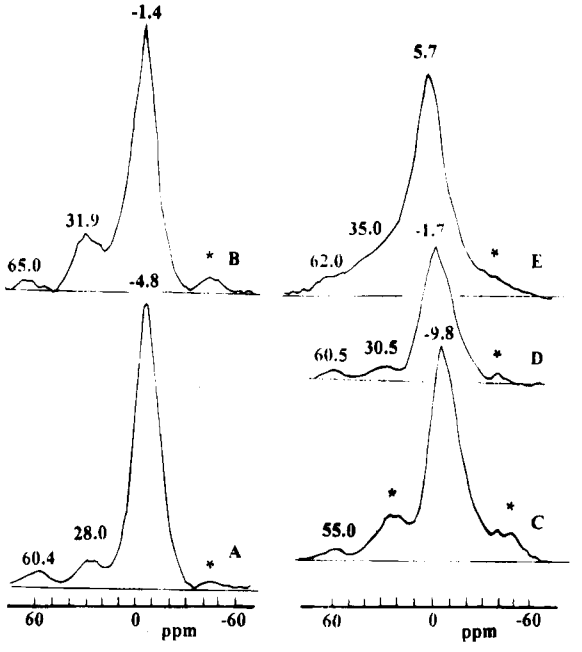

Figure 6. ^{27}Al MAS-NMR spectra of aluminum oligomer intercalated α-SnP and α-ZrP materials and Al^{3+}-exchanged α-ZrP: (A) Al_{13}−SnP; (B) Ac−SnP; (C) Al^{3+}-exchanged α-ZrP; (D) CHL−ZrP; (E) Ac−ZrP. Asterisks denote spinning side bands.

^{31}P in α-ZrP derivatives appears at −26.2 ppm (CHL−ZrP) and −24.1 (Ac−ZrP). The net variation of the chemical shift is again higher in α-ZrP than in α-SnP.

^{27}Al MAS-NMR. The ^{27}Al MAS-NMR spectra of the studied samples are shown in Figures 6 and 7. The Al_{13}−SnP intercalate (Figure 6A) presents the signals of octahedral aluminum at −4.8 ppm and of tetrahedral aluminum at 60.4 ppm. A third signal at 28.0 ppm with similar intensity to that of AlO_4 also appears in this spectrum. This signal cannot be considered only as a spinning side band, as its intensity and position depend on the amount and on the type of Al oligomer intercalated. It has been assigned to pentacoordinated Al.[20-23] The position of the signals varies with the type of Al oligomer intercalated. Indeed, for sample Ac−SnP (Figure 6B) the peaks

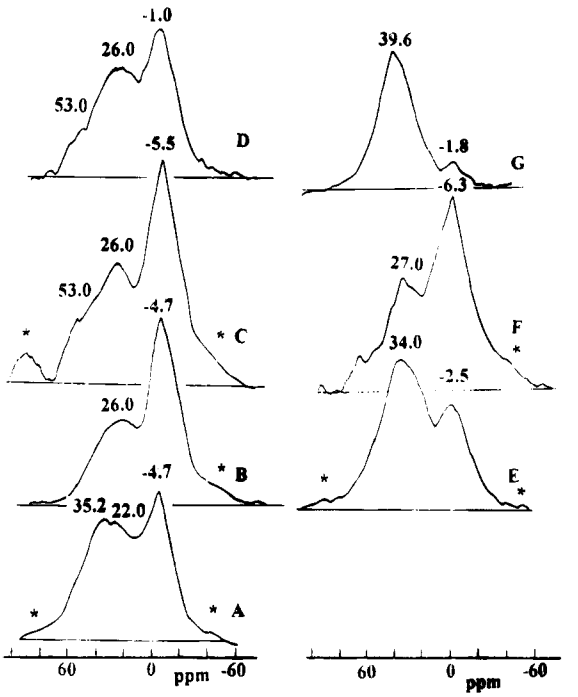

Figure 7. ^{27}Al MAS-NMR spectra of aluminum oxide-pillared α-SnP and α-ZrP materials (400 °C): (A) Al_{13}−SnP; (B) CHL−SnP; (C) Ac−SnP; (D) Al_{13}−SnP + NH_3; (E) CHL−ZrP; (F) Ac−ZrP; (G) CHL−ZrP + NH_3. Asterisks denote spinning side bands.

appear at −1.4, 65.0, and 31.9 ppm. The intensity of the peak near 30 ppm is higher in Ac−SnP (Figure 6B) than in Al_{13}−SnP (Figure 6A). However, a quantitative estimation of the band intensity is difficult because of the superposition of the main signals with the spinning side bands.

The ^{27}Al spectrum of Al^{3+}-exchanged α-ZrP (Figure 6C) shows the characteristic signal of octahedral aluminum at −9.8 ppm, together with a small peak at 55.0 ppm. The spectra corresponding to aluminum oligomer intercalated α-ZrP materials (Figure 6D,E) also exhibit the characteristic signals of AlO_6 and AlO_4 environments (broad peaks), together with a resonance at 30.5 ppm (CHL−ZrP) or at 35.0 ppm (Ac−ZrP).

Upon calcination at 400 °C (Figure 7), the intensity of the resonance located between 20 and 40 ppm is significantly enhanced and broadened. In the case of sample Al_{13}−SnP, a band with maxima at 22.0 and 35.2 ppm is detected (Figure 7A). In the spectrum of sample CHL−SnP, the band has a maximum at 26.0 ppm (Figure 7B), and in that of sample Ac−SnP, an asymmetric band formed by two components at 26 and 53 ppm is detected (Figure 7C). In all the calcined α-SnP intercalated materials, the signal of regular tetrahedral Al (at about 60 ppm) is weak. In the spectrum of CHL−ZrP, the band at 34 ppm is significantly more intense than that corresponding to octahedral aluminum (−2.5 ppm) (Figure 7E). Conversely, in the spectrum of Ac−ZrP (Figure 7F) the signal of octahedral Al is the most intense.

A flow of ammonia passed through the sample CHL−ZrP (Figure 7G) results in a considerable diminution of the octahedral component near −2 ppm, whilst in the case of sample Al_{13}−SnP (Figure 7D) the spectrum is not practically modified.

Discussion

In general, the ^{31}P NMR signal of layered phosphates shifts toward higher field with increasing connectivity of phosphorus (Q^n) and decreasing electronegativity of the framework metal cation. In both phosphates, each phosphorus is connected to three metal centers by bridging oxygens. Therefore, the position

of the chemical shifts is directly related to the Allred–Rochow electronegativity (Sn, 1.72; Zr, 1.22), as proposed by Hudson and Workman.[19] Phosphorus in α-ZrP has a higher electron density than in α-SnP, suggesting that α-SnP must be more acidic than α-ZrP.

The solution chemistry of aluminum has been studied in detail by ^{27}Al NMR.[24] The predominant species in the aluminum solution partially neutralized with NaOH is the tridecameric ion $[AlO_4Al_{12}(OH)_{24}(H_2O)_{12}]^{7+}$ or (Al_{13}). This ion is also found in CHL solutions together with other species.[5] From the ^{31}P NMR results, an increasing coverage of the phosphate surface (as measured by the intensity ratio I_2/I_1) by aluminum oligomers has been detected, which is consistent with the presence of increasing amounts of aluminum. However, although the aluminum content of the CHL–SnP intercalate is more than twice as much as that of Al_{13}–SnP, the surface coverage only slightly increases from 60% (Al_{13}–SnP) to 65% (CHL–SnP). Assuming the layer thickness of the phosphate to be 6.5 Å, the basal expansion in Al_{13}–SnP (10.5 Å) is consistent with the presence of a monolayer of Al_{13} species in the interlayer region, as this cation has a long axis of *ca.* 10 Å. Incorporation of more aluminum in dialyzed Al_{13}–SnP than in centrifuged Al_{13}–SnP (both phases have the same interlayer distance) must be due to the fact that the intercalated species in the former have a lower charge. Therefore, more phosphate groups participate in the interaction with the aluminum oligomer. It is known that dialysis leads to a better reorganization of the oligomers on the host surface. Then, with this method, a more homogeneous material with sharper diffraction lines is obtained. In the XRD pattern of CHL–SnP, a broad peak is observed, which corresponds to a basal expansion of 18.1 Å, and is consistent with the existence of a bilayer of Al_{13} oligomers in the interlayer space of α-SnP.

Oligomer condensation occurs when the intercalation reaction is performed under reflux,[10] thus facilitating the formation of larger species inside the interlayers, as evidenced by XRD (Table 1). Fu *et al.*[25] have recently identified by NMR two new polyoxycation clusters formed by polymerization of Al_{12} units from an Al_{13} solution treated at high temperature. Thus, in Ac–SnP, a dimeric Keggin ion, possibly Al_{24}, rather than a bilayer of Al_{13} could possibly have been intercalated, as the basal expansion of the calcined product (13.7 Å) is twice the value observed for the calcined CHL–SnP sample. The surface covered in Ac–SnP is practically 100%.

In CHL–ZrP, more than one species is intercalated. The XRD pattern of this intercalate shows a main peak at 18.9 Å and a small diffraction peak at 13.7 Å. The basal expansion corresponding to the main peak is 5.7 Å lower than that of CHL–SnP, suggesting the presence of a monolayer of Al_{13} species or similar oligomers, but with a lower charge, as all the phosphates tetrahedra interact with the Al polyoxocations. The presence of small Al species cointercalated cannot be ruled out, which may contribute to increase the basal spacing from the expected value (~17 Å) to the observed one (18.9 Å). That different intercalates of CHL for each phosphate are obtained indicates that the host surface may modify the nature of the intercalated oligomer. In the case of Ac–ZrP, a high basal spacing as in the Ac–SnP intercalate is observed, but not all the phosphorus tetrahedra interact to the same extent with the Al oligomer.

Calcination of the intercalates leads to pillared phosphates maintaining basal expansions between 5.3 and 13.7 Å (Table 1). As the structural environment of P does not change in the phosphate layer, the upfield shift of the ^{31}P signal in pillared materials must be ascribed to the interaction of phosphate with aluminum oligomers, probably by formation of P–O–Al bonds. The stronger interaction observed in α-ZrP is related to the more basic nature of the phosphate groups in this compound as compared with α-SnP. The position of the ^{31}P chemical shift in pillared α-ZrP materials is similar to that observed in AlPO compounds, namely, near −26 ppm.[26]

In the ^{27}Al spectra of the aluminum oligomer intercalated phosphates, three signals are apparent in ranges of chemical shifts corresponding to AlO_4, 60–65 ppm; AlO_5, 28–35 ppm; and AlO_6, −10 to +6 ppm.[27] The predominant signal is that of octahedral aluminum, i.e. Al ions surrounded by OH groups and water molecules. The intensity of the signals near 30 and 60 ppm is relatively low. Upon calcination, most OH groups of the intercalated oligomer are removed, so that the aluminum ions near the phosphate layer may share oxygens with phosphorus tetrahedra. As phosphorus atoms are separated by approximately 5 Å, each aluminum can only link to one phosphate group. Moreover, it can be expected that aluminum bonded to a phosphate layer exhibits intermediate low-symmetry coordinations, favoring the detection of the pentacoordinated Al component. However, a broad peak centered at *ca.* 30 ppm could not be final evidence for Al pentacoordination, inasmuch as distorted tetrahedral aluminum may also give rise to this resonance.[28] Unfortunately, from modified Auger parameter values obtained in this work, it was not possible to infer the presence of Al^V on the pillared phosphate surfaces, as Al^{VI} is also present. In fact, Al^V and Al^{VI} could not be discriminated by XPS in andalusite.[29]

The signal of pentacoordinated aluminum bonded to phosphate ions in solution is found between 43 and 52 ppm.[30] However, in a solid, there must be a wide range of interactions, and hence, a broad line in the region of the spectra between 20 and 50 ppm would be expected. The signal attributed to pentacoordinated aluminum increases in the samples calcined at 400 °C and shifts toward higher field, as a consequence of the increasing interaction with the phosphate layer.

The proportion of pentacoordinated aluminum in the calcined products depends on the basal spacing and on the phosphate used. In the materials studied here, the intensity ratio of octahedral to pentacoordinate aluminum increases with the basal spacing. This may justify that the linkage of the aluminum oxyhydroxide to the phosphate layer is established through aluminum ions occupying AlO_5 environments, whereas the remaining aluminum ions occupy octahedral positions in the oxide props pillaring two adjacent phosphate layers. The fact that the concentration of pentacoordinated aluminum is not reduced upon adsorption of ammonia supports the hypothesis that the AlO_5 environment is stabilized by its interaction with the phosphate layer and cannot be broken by interaction with ammonia. Instead, the coordination of central Al in the pillar changes from octahedral to pentacoordinate.

The concentration of pentacoordinated aluminum is much higher in pillared α-ZrP than in pillared α-SnP. For instance, Al^V is the predominant component in CHL–ZrP calcined at 400 °C, despite that the basal spacing of this material (13.7 Å) is practically identical to that of CHL–SnP calcined at the same temperature (13.8 Å). Given that the interaction between aluminum and the phosphate layer is stronger in α-ZrP than in α-SnP, it seems that the framework of the intercalated aluminum oxyhydroxide tends to spread in the interlayer of α-ZrP, favoring more aluminum ions to interact with the zirconium phosphate surface, and hence, it would justify that stuffed pillared structures with low surface areas are formed in this phosphate.

Concluding Remarks

Aluminum oxide-pillared α-tin and α-zirconium phosphates have been prepared by intercalation of aluminum oligomers and subsequent calcination at 400 °C.

In addition to octahedral Al, an unusually high concentration of possibly pentacoordinated Al has been detected in these pillared materials. From MAS-NMR data, the strong interaction established between the interlayer aluminum oxide and the phosphate layer seems to be due to the formation of $Al^{V}-O-P$ bonds, whilst octahedral Al would occupy intermediate positions in the oxide props. Auger-modified parameter values have been measured for the pillared phosphates, but unfortunately, AlO_5 and AlO_6 environments could not be discriminated from these data. The proportion of Al directly linked to the phosphate layer is higher in α-ZrP than in α-SnP, which gives rise to the formation of stuffed pillared structures in the former phosphate.

Acknowledgment. This research was supported by the CICYT (Spain) Project MAT94-0678 and by the C. E. Programme BRITE-EURAM Contract BRE2-CT93-0450. Thanks are due to Dr. R. T. C. Slade (University of Exeter) for critical reading of the manuscript.

References and Notes

(1) Clearfield, A.; Roberts, B. D. *Inorg. Chem.* **1988**, *27*, 3237.
(2) Olivera-Pastor, P.; Jiménez-López, A.; Maireles-Torres, P.; Rodríguez-Castellón, E.; Alagna, L.; Tomlinson, A. A. G. *J. Chem. Soc., Chem. Commun.* **1989**, 751.
(3) Cheng, S.; Wang, T. C. *Inorg. Chem.* **1989**, *28*, 1283.
(4) Deng, Z.; Lambert, J. F. H.; Fripiat, J. *J. Chem. Mat.* **1989**, *1*, 640.
(5) Lalik, E.; Kolodziejski, W.; Lerf, A.; Klinowski, J. *J. Phys. Chem.* **1993**, *97*, 223.
(6) Tanaka, H.; Takahashi, J.; Tsuchiya, J.; Kobayashi, Y.; Kurokawa, Y. *J. Non-Cryst. Solids* **1989**, *109*, 164.
(7) Figueras, F. *Catal. Rev.-Sci. Eng.* **1988**, *30*, 457.
(8) Guerrero-Ruíz, A.; Rodríguez-Ramos, I.; Fierro, J. L. G.; Jiménez-López, A.; Olivera-Pastor, P.; Maireles-Torres, P. *Appl. Catal., A* **1992**, *92*, 81.
(9) Clearfield, A. *Comments Inorg. Chem.* **1990**, *10*, 89.
(10) Jiménez-López, A.; Maireles-Torres, P.; Olivera-Pastor, P.; Rodríguez-Castellón, E.; Tomlinson, A. A. G. In *Multifunctional Mesoporous Inorganic Solids*; Sequeira, C. A. C., Hudson, M. J., Eds.; Kluwer Academic Publishers: Amsterdam, 1993; p 273.
(11) Maireles-Torres, P.; Olivera-Pastor, P.; Rodríguez-Castellón, E.; Jiménez-López, A.; Tomlinson, A. A. G.; Perez, G.; Keheyan, Y. European Pat. RM 92A000376, 1992.
(12) Maireles-Torres, P.; Olivera-Pastor, P.; Rodríguez-Castellón, E.; Jiménez-López, A.; Alagna, L.; Tomlinson, A. A. G. *J. Mater. Chem.* **1991**, *1*, 319.
(13) Alberti, G.; Torracca, E. *J. Inorg. Nucl. Chem.* **1968**, *30*, 317.
(14) Costantino, U.; Gasperoni, A. *J. Chromatogr.* **1970**, *51*, 289.
(15) Alberti, G.; Casciola, M.; Costantino, U. *J. Colloid. Interface Sci.* **1985**, *107*, 256.
(16) Remy, M. J.; Genet, M. J.; Poncelet, G.; Lardinois, P. F.; Notte, P. P. *J. Phys. Chem.* **1992**, *96*, 2614.
(17) (a) Wagner, C. D.; Passoja, D. E.; Hilery, H. F.; Kinisky, T. G.; Six, H. A.; Jansen, W. T.; Taylor, J. A. *J. Vac. Sci. Technol.* **1982**, *21* (4), 933. (b) Wagner, C. D. In *Practical Surface Analysis*; Briggs, E. D., Seah, M. P., Eds.; J. Wiley: New York, 1990; Vol. 1, pp 595–634.
(18) Remy, M. J.; Jenet, M. J.; Notte, T. P.; Lardinois, T. F.; Poncelet, G. *Microporous Mater.* **1993**, *2*, 7.
(19) Hudson, M. J.; Workman, A. D. *J. Mater. Chem.* **1991**, *1*, 375.
(20) Dupree, R.; Farnan, I.; Forty, A. J.; El-Mashri, S.; Bottyan, L. *J. Phys., Paris* **1985**, *46*, C8–113.
(21) Gilson, J. P.; Edwards, G. C.; Peters, A. W.; Rajagopalan, K.; Wormsbecher, R. F.; Roberie, T. G.; Shatlock, M. P. *J. Chem. Soc., Chem. Commun.* **1987**, 91.
(22) Slade, R. C. T.; Southern, J. C.; Thomson, I. M. *J. Mater. Chem.* **1991**, *1*, 563.
(23) Nazar, L. F.; Fu, G.; Bain, A. D. *J. Chem. Soc., Chem. Commun.* **1992**, 251.
(24) Akitt, J. W.; Farthing, A. *J. Chem. Soc., Dalton Trans.* **1981**, 1606.
(25) Fu, G.; Nazar, L. F.; Bain, A. D. *Chem. Mater.* **1991**, *3*, 602.
(26) Sanz, J.; Campelo, J. M.; Marinas, J. M. *J. Catal.* **1991**, *130*, 642.
(27) Engelhardt, G.; Michel, D. In *High Resolution Solid State NMR of Silicates and Zeolites*; Wiley, Chichester, 1987.
(28) Samoson, A.; Lippmaa, E.; Englehardt, G.; Lohse, U.; Jerschkewits, H. G. *Chem. Phys. Lett.* **1986**, *134*, 589.
(29) West, R. H.; Castle, J. E. *Surf. Interface Anal.* **1982**, *4*, 68.
(30) Mortlock, R. F.; Bell, A. T.; Radke, C. J. *J. Phys. Chem.* **1993**, *97*, 775.

JP941233D